

# Heat and mass transfer of two immiscible flows of Jeffrey fluid in a vertical channel

Shreedevi Kalyan<sup>1</sup>  | Ashwini Sharan<sup>1</sup> | Ali J. Chamkha<sup>2</sup>

<sup>1</sup>Department of Mathematics,  
Sharnbasva University, Kalaburagi,  
Karnataka, India

<sup>2</sup>Faculty of Engineering, Kuwait College  
of Science and Technology, Kuwait,  
Doha District, Kuwait

## Correspondence

Shreedevi Kalyan, Department of  
Mathematics, Sharnbasva University,  
Kalaburagi 85103, Karnataka, India.  
Email: [kalyanshreedevi@gmail.com](mailto:kalyanshreedevi@gmail.com)

## Abstract

In this article, we examined the effect of heat and mass transfer flow of two immiscible Jeffrey fluids in a vertical channel. The highly nonlinear coupled ordinary differential equations are evaluated using regular perturbation parameters, for small values of perturbation parameter. The effect of Jeffrey's parameter on the flow and the effects of various physical parameters entering into the problem on dimensionless velocity, temperature, and concentration distribution is illustrated graphically. We observe that the Jeffrey parameter, thermal, and mass Grashof number enhance the fluid flow, while the chemical reaction parameter suppresses the fluid flow, also it is established that the Nusselt number is boosted by enhancing the thermal and mass Grashof number. We observed that the results are in very good agreement with the results obtained for a viscous fluid.

## KEYWORDS

chemical reaction and two phase flow, free convective flow, heat and mass transfer, Jeffrey fluid

## 1 | INTRODUCTION

The flow of fluids is studied in mechanical engineering and is highly advanced in chemical and civil engineering. In real life, the most common use of liquids by hydroelectric industries is water, and water is used to produce electricity on a large scale, in cars: power generation, cooling engine, and lubrication. Air conditioners, refrigerators, and heat energy industries are important fields while water is used as an active liquid. In a real situation, many industrial fluids such as ketchup, pastes, slurries, paint, shampoo, blood, glues, printing inks, food

materials, soap and detergent slurries, and polymer solutions are non-Newtonian in nature. These fluids are basically nonlinear. The constitutive equations relating to such fluids are intrinsically more sophisticated than conventional Newtonian (Navier–Stokes) fluids. Most non-Newtonian models (Maxwell models, Oldroyd-B models, Walters-B short memory models, Jeffrey model, Eyring–Powell models, etc.) involve varying degrees of refinement to the classical momentum conservation equations. Out of these, the Jeffrey model is the simplest one rate type non-Newtonian liquids which exhibit shear diminishing attributes, yield pressure, and high shear viscosity. The presence of various fluids The arrangement of fluids arises due to varying temperatures and differences in concentration. The method of conveying heat and weight in parallel is tested by the effect stratification medium in both hot and concentrated micropolar fluids in the convective transport in real-world conditions.

The Newtonian fluid and Jeffrey fluid models attracted several researchers to compile the Newtonian fluid model, which can be found in the previous case as a special case, and the physiological fluid and Jeffrey fluid are found to be the best model. Under various circumstances, many analysts have read about Jeffrey's parameter fluid studied by Hayat et al.<sup>1</sup> Under heat transfer under the influence of the peristaltic flow of Jeffrey fluid is investigated by Vajravelu et al.<sup>2</sup> Jyothi et al.<sup>3</sup> analyzed the flow in the Jeffrey fluid tubes with small diameters in the holes of the two liquid models. Kothandapani and Srinivas<sup>4</sup> have studied the peristaltic transport of a Jeffrey fluid under the magnetic field, and Pandey et al.<sup>5</sup> observed the unsteady transport behavior. Santhosh et al.<sup>6</sup> found that a circular tube inserted inside has the property of a microstructure blown by the Jeffrey liquid flow. Anu Nair et al.<sup>7</sup> checked how to analyze the transfer of natural flux flow in a vertical channel from a horizontal plate and described in detail the relationship between the Nusselt number and the Rayleigh number excluding the plate types. Anu Nair and Karuppasamy<sup>8</sup> and Anu Nair et al.<sup>9</sup> have been tested to determine the value of  $C$  in the Nusselt number of new methods such as the Small Square methods and the Bayesian methods (i.e., Development Method). Heat transfer and free convection flow to the left wall due to sources in the square enclosure were investigated by Anu Nair et al.<sup>10</sup> and Anu Nair and Karuppasamy.<sup>11</sup> Since Ebenezer et al.<sup>12</sup> determine temperature by number even though it controls the temperature of the local temperature converter from the corresponding contaminants to a single phase to increase the average temperature. An important literature review of Jeffrey's water flow has made by Bird and coauthors and Hayat and coauthors.<sup>13–18</sup>

Flow rate analysis includes the internal flow of two phases, isothermal compressible flow, non-Newtonian, Newtonian incompressible fluids, external flow, and adiabatic flow, in a porous medium. Prasence of convective fluid, micropolar fluid and its growth has been studied in the literature.<sup>19–22</sup>

Prathap Kumar et al.<sup>23</sup> have studied that the micropolar with Newtonian fluid in a fully developed free convective is read in a vertical channel. In heat transfer problems many effective efforts have been done for solving different types of problems, different authors have used homotopy perturbation method in oscillatory flow and fluid flow.<sup>24–28</sup> Research has been done in the presence of magnetic and electric fields. Malashetty et al.<sup>29</sup> investigated the magnetoconvection of two immiscible fluids in a vertical enclosure. Major problems in nonlinear homotopy analysis method-related nonlinear fluids are first investigated in the literature seen in Hayat and coauthors.<sup>30–36</sup>

Harish Babu and coauthors<sup>37–39</sup> studied the magneto hydrodynamic (MHD) heat and mass transfer of a Jeffrey fluid over a stretching sheet with chemical reaction and thermal radiation.

Harish Babu and coauthors<sup>40–43</sup> analyzed the effects on MHD Jeffrey nanofluid, but very little work is done in the presence of first-order chemical research.

Motivated by these facts, a mathematical model of heat and mass transfer of two immiscible flows of Jeffrey fluid in a vertical channel has been studied. Present results not only find applications in realistic engineering but also assist as a complement to the earlier research works.

## 2 | MATHEMATICAL FORMULATION

Considering a two-dimensional steady laminar free convective flow over an isothermal inclined plate the problem is described in a vertical channel, it is assumed that both the walls (left wall and right wall) are maintained at different wall temperatures and concentrations excluding the density (Figure 1).

The coupled nonlinear governing equations of conservation of momentum equation, conservation of energy, and concentration can be written as<sup>6</sup>

*Region-I*

$$\rho_1 g \beta_{T1} (T_1 - T_{w2}) + \rho_1 g \beta_{C1} (C_1 - \bar{C}_2) + \frac{\mu_1}{(1 + \lambda_1)} \frac{d^2 U_1}{dY^2} - \frac{dp}{dX} = 0, \quad (1)$$

$$\frac{d^2 T}{dY^2} = - \frac{v_1}{\alpha_1 C_p} \left( \frac{dU_1}{dY} \right)^2, \quad (2)$$

$$D_1 \frac{d^2 T_1}{dY^2} - K_1 C_1 = 0. \quad (3)$$

*Region-II*

$$\rho_2 g \beta_{T2} (T_2 - T_{w2}) + \rho_2 g \beta_{C2} (C_2 - \bar{C}_2) + \frac{\mu_2}{(1 + \lambda_2)} \frac{d^2 U_2}{dY^2} - \frac{dp}{dX} = 0, \quad (4)$$

$$\frac{d^2 T_2}{dY^2} = - \frac{v_2}{\alpha_2 C_p} \left( \frac{dU_2}{dY} \right)^2, \quad (5)$$

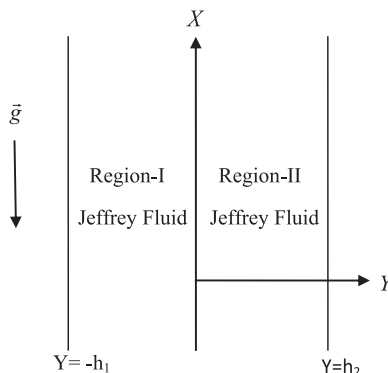


FIGURE 1 Physical configuration

$$D_2 \frac{d^2 C_2}{dy^2} - K_2 C_2 = 0. \quad (6)$$

The physical conditions for boundary and interface for this mathematical formulation for velocity, temperature, and concentration are given by

$$U_1(-h_1) = 0, \quad U_2(h_2) = 0, \quad U_1(0) = U_2(0), \quad \frac{\mu_1}{(1 + \lambda_1)} \frac{dU_1}{dY}(0) = \frac{\mu_2}{(1 + \lambda_2)} \frac{dU_2}{dY}(0),$$

$$T_1(-h_1) = Tw_1, \quad T_2(h_2) = Tw_2, \quad T_1(0) = T_2(0), \quad \frac{dT_1}{dY}(0) = \frac{dT_2}{dY}(0),$$

$$C_1(-h_1) = \bar{C}_1, \quad C_2(h_2) = \bar{C}_2, \quad C_1(0) = C_2(0), \quad D_1 \frac{dC_1}{dY}(0) = D_2 \frac{dC_2}{dY}(0). \quad (7)$$

Introduce the following nondimensional parameters:

$$u_i = \frac{U_i}{\bar{U}_1}, \quad y_i = \frac{Y_i}{h_i}, \quad \theta_1 = \frac{T_1 - T_{w2}}{T_{w1} - T_{w2}}, \quad \theta_2 = \frac{T_2 - T_{w2}}{T_{w1} - T_{w2}}, \quad \phi_1 = \frac{C_1 - \bar{C}_2}{\bar{C}_1 - \bar{C}_2},$$

$$\phi_2 = \frac{C_2 - \bar{C}_2}{\bar{C}_1 - \bar{C}_2}, \quad Gc = \frac{g\beta_{C1} h_1^3 (\bar{C}_1 - \bar{C}_2)}{\nu_1^2}, \quad Gr = \frac{g\beta_{T1} h_1^3 (T_{w1} - T_{w2})}{\nu_1^2}, \quad Re = \frac{\bar{U}_1 h_1}{\nu_1},$$

$$p = \frac{h_1^2}{\mu_1 \bar{U}_1} \frac{dp}{dX}, \quad Br = \frac{\nu_1 \bar{u}_1^2}{\alpha_1 C_p \Delta T} \left( \frac{dU_1}{dY} \right)^2. \quad (8)$$

Substituting the transformations (8) into Equations (1)–(6) we get  
*Region-I*

$$\frac{d^2 \phi_{10}}{dy} + (1 + \lambda_1) G_1 \theta_1 + (1 + \lambda_1) G_2 \phi_2 - (1 + \lambda_1) p = 0, \quad (9)$$

$$\frac{d^2 \theta_1}{dy} = 0, \quad (10)$$

$$\frac{d^2 \phi_1}{dy} - \alpha_1^2 \phi_1 = 0. \quad (11)$$

*Region-II*

$$\frac{d^2 u_2}{dy^2} + (1 + \lambda_2) a_2 \theta_2 + (1 + \lambda_2) a_2 \phi_2 - (1 + \lambda_2) m h^2 p = 0, \quad (12)$$

$$\frac{d^2 \theta_2}{dy^2} = 0, \quad (13)$$

$$\frac{d^2 \phi_2}{dy} - \alpha_2^2 \phi_2 = 0. \quad (14)$$

The nondimensional form of boundary and interface conditions of Equation (7) becomes

$$u_1(-1) = 0, \quad u_2(1) = 0, \quad u_1(0) = u_2(0), \quad \frac{1}{(1 + \lambda_1)} \frac{du_1}{dy}(0) = \frac{1}{(1 + \lambda_2)} \frac{1}{mh} \frac{du_2}{dy}(0),$$

$$\theta_1(-1) = 1, \quad \theta_2(1) = 0, \quad \theta_1(0) = \theta_2(0), \quad \frac{d\theta_1}{dy}(0) = \frac{1}{kh} \frac{d\theta_2}{dy}(0),$$

$$\phi_1(-1) = 1, \quad \phi_2(-1) = 0, \quad \phi_1(0) = \phi_2(0), \quad \frac{d\phi_1}{dy}(0) = \frac{d}{h} \frac{d\phi_2}{dy}(0), \quad (15)$$

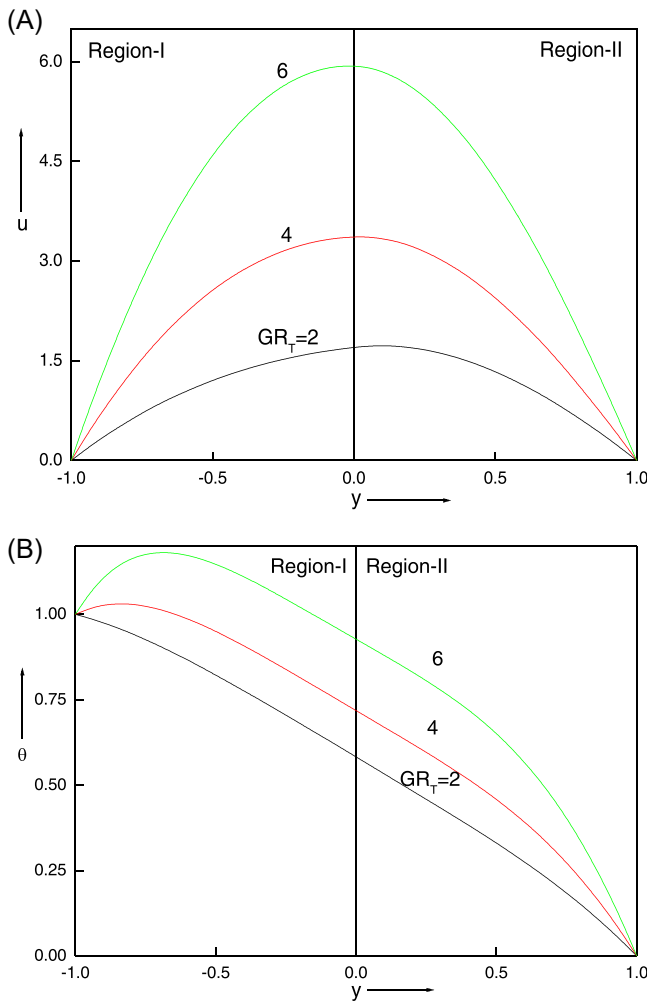


FIGURE 2 (A) Velocity profiles for different values of thermal Grashof number  $Gr_t$ . (B) Temperature profiles for different values of thermal Grashof number  $Gr$ . [Color figure can be viewed at [wileyonlinelibrary.com](https://onlinelibrary.wiley.com)]

where

$$G_1 = \frac{Gr}{Re}, \quad G_2 = \frac{Gc}{Re}, \quad h = \frac{h_2}{h_1}, \quad m = \frac{\mu_1}{\mu_2}, \quad b_t = \frac{\beta_{T2}}{\beta_{T1}}, \quad b_c = \frac{\beta_{C2}}{\beta_{C1}}, \quad n = \frac{\rho_2}{\rho_1}.$$

## 3 | METHOD OF SOLUTIONS

### 3.1 | Perturbation method

The coupled nonlinear governing differential Equations (9)–(14) with the appropriate boundary and interface conditions (15) are solved analytically using the regular perturbation method for the small values perturbation parameter ( $Br = \varepsilon$  is the perturbation parameter). Differential equations are first decomposed to a system of zeroth- and first-order equations corresponding to Region-I and Region-II. We assume the solutions in the form as follows:

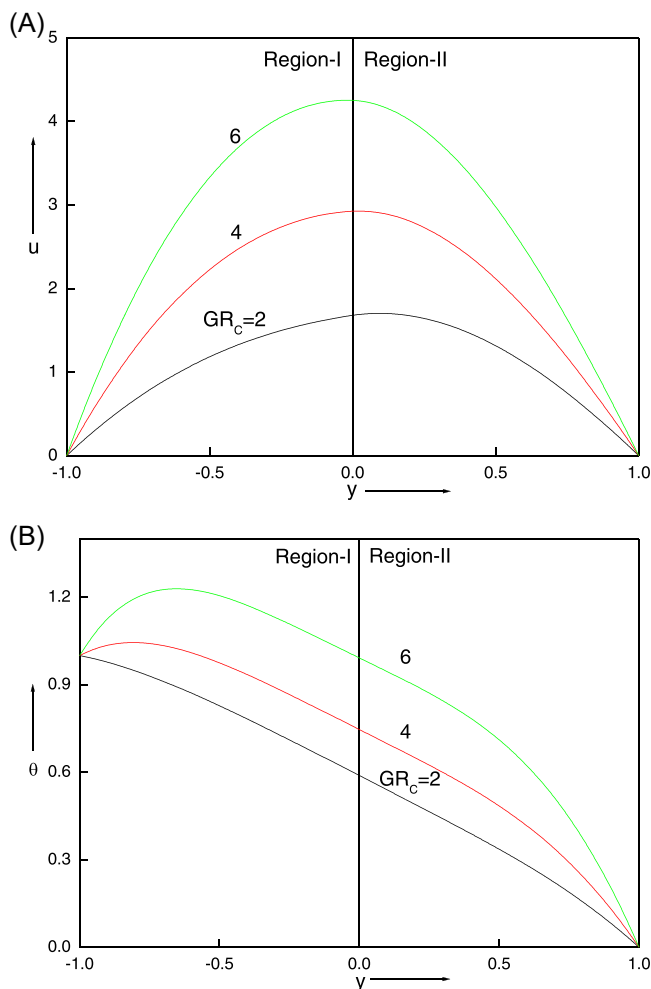


FIGURE 3 (A) Velocity profiles for different values of mass Grashof number  $Gr_c$ . (B) Temperature profiles for different values of mass Grashof number  $Gr_c$ . [Color figure can be viewed at [wileyonlinelibrary.com](https://wileyonlinelibrary.com)]

$$(u_1, \theta_1) = (u_{10}, \theta_{10}) + \varepsilon(u_{11}, \theta_{11}) + \dots, \quad (16.1)$$

$$(u_2, \theta_2) = (u_{20}, \theta_{20}) + \varepsilon(u_{21}, \theta_{21}) + \dots, \quad (16.2)$$

where  $u_{10}, u_{20}, \theta_{10}, \theta_{20}$  are solutions for the case  $\varepsilon = 0$  and  $u_{11}, u_{21}, \theta_{11}, \theta_{21}$  are corrections to the zeroth-order quantities. Substituting (16.1) and (16.2) into (9)–(14) and equating the like powers of  $\varepsilon$  to zero and one, yield the following set of equations:

*Region-I*

Zeroth-order equations

$$\frac{d^2 u_{10}}{dy^2} + (1 + \lambda_1)G_1 \theta_{10} + (1 + \lambda_1)G_2 \phi_1 - (1 + \lambda_1)p = 0, \quad (17)$$

$$\frac{d^2 \theta_{10}}{dy^2} = 0, \quad (18)$$

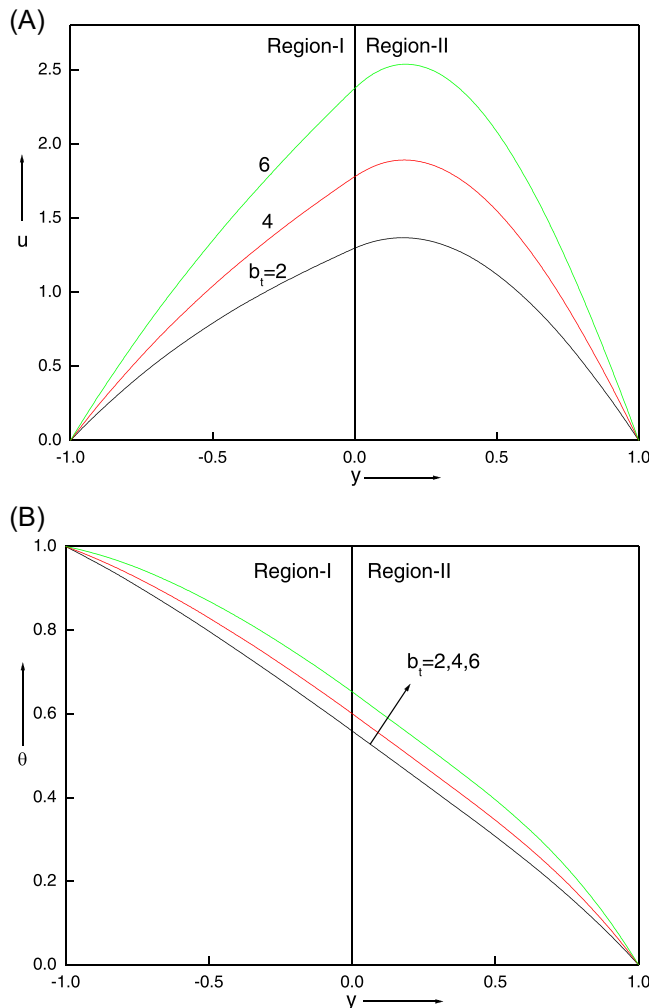


**FIGURE 4** (A) Velocity profiles for different values of thermal expansion ratio  $b_t$ . (B) Temperature profiles for different values of thermal expansion ratio  $b_t$ . [Color figure can be viewed at [wileyonlinelibrary.com](https://onlinelibrary.wiley.com)]

$$\frac{d^2\phi_1}{dy^2} - \alpha_1^2\phi_1 = 0. \quad (19)$$

First-order equations

$$\frac{d^2u_{11}}{dy^2}(0) + (1 + \lambda_1)G_1\theta_{11} = 0, \quad (20)$$

$$\frac{d^2\theta_{11}}{dy^2} + \left(\frac{du_{10}}{dy}\right)^2 = 0. \quad (21)$$

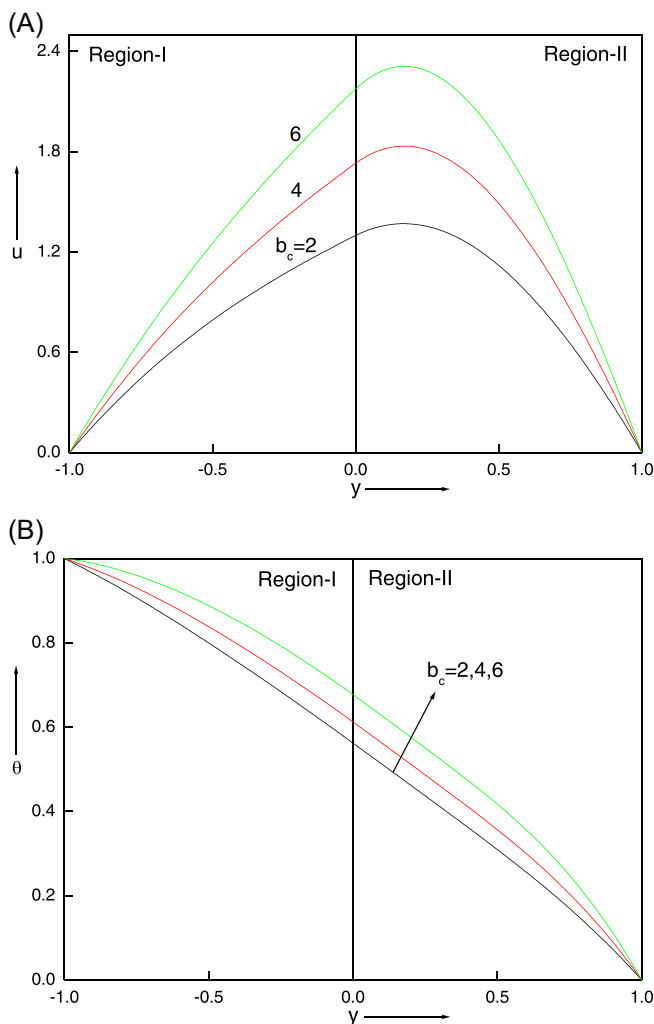


FIGURE 5 (A) Velocity profiles for different values of concentration expansion ratio  $b_c$ . (B) Temperature profiles for different values of concentration expansion ratio  $b_c$ . [Color figure can be viewed at [wileyonlinelibrary.com](https://wileyonlinelibrary.com)]

## Region-II

## Zeroth-order equations

$$\frac{d^2 u_{20}}{dy^2} = (1 + \lambda_2) a_1 \theta_{20} + (1 + \lambda_2) a_2 \phi_2 + (1 + \lambda_2) m h^2 p, \quad (22)$$

$$\frac{d^2 \theta_{20}}{dy^2} = 0, \quad (23)$$

$$\frac{d^2 \phi_2}{dy^2} - \alpha_2^2 \phi_2 = 0. \quad (24)$$

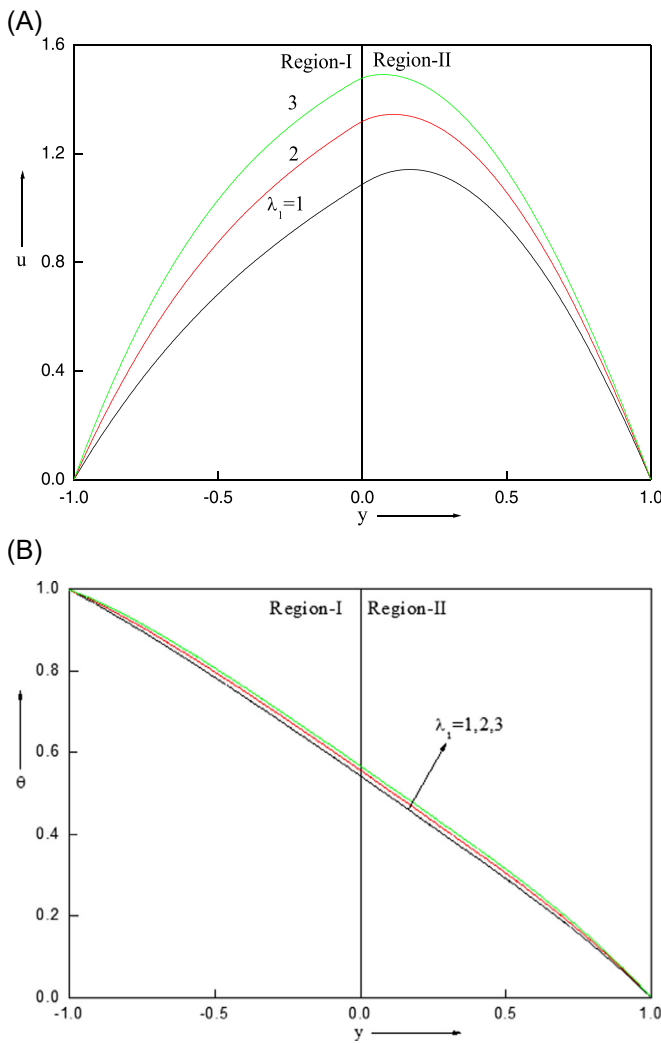


FIGURE 6 (A) Velocity profiles for different values of Jeffrey parameter  $\lambda_1$ . (B) Temperature profiles for different values of Jeffrey parameter  $\lambda_1$ . [Color figure can be viewed at [wileyonlinelibrary.com](http://wileyonlinelibrary.com)]

## First-order equations

$$\frac{d^2 u_{21}}{dy^2} = (1 + \lambda_2) a_1 \theta_{21}, \quad (25)$$

$$\frac{d^2 \theta_{21}}{dy^2} - a_3 \left( \frac{du_{20}}{dy} \right)^2 = 0. \quad (26)$$

## Zeroth-order conditions

$$u_{10}(-1) = 0, \quad u_{20}(1) = 0, \quad u_{10}(0) = u_{20}(0), \quad (1 + \lambda_2) \frac{du_{10}}{dy}(0) = \frac{(1 + \lambda_1)}{mh} \frac{du_{20}}{dy}(0),$$

$$\theta_{10}(-1) = 1, \quad \theta_{20}(1) = 1, \quad \theta_{10}(0) = \theta_{20}(0), \quad \frac{d\theta_{10}}{dy}(0) = \frac{1}{kh} \frac{d\theta_{20}}{dy}(0),$$

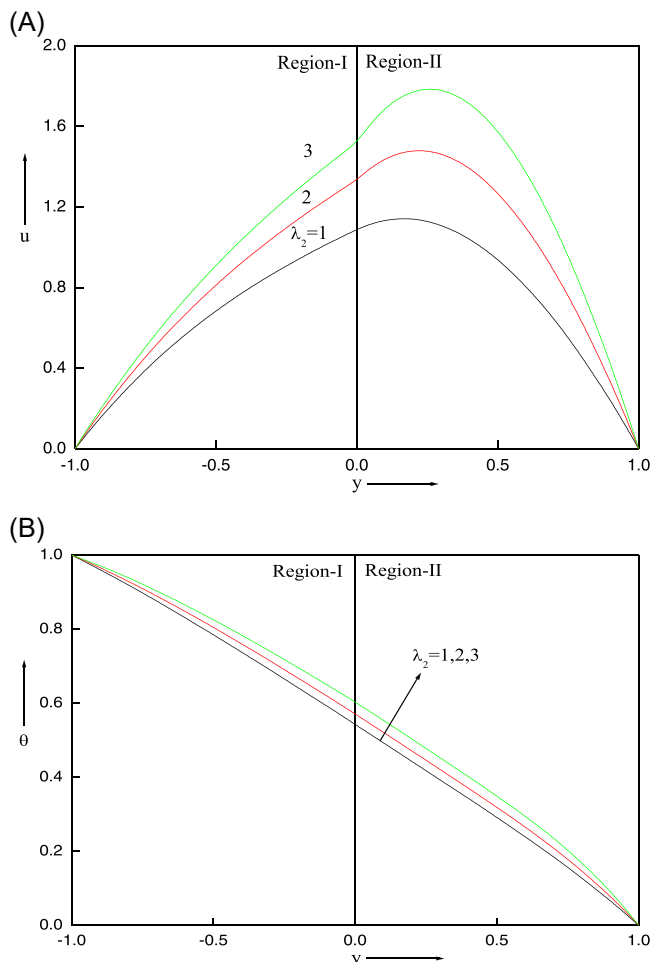


FIGURE 7 (A) Velocity profiles for different values of Jeffrey parameter  $\lambda_2$ . (B) Temperature profiles for different values of Jeffrey parameter  $\lambda_2$ . [Color figure can be viewed at [wileyonlinelibrary.com](https://onlinelibrary.wiley.com/doi/10.1002/htj.22694)]

$$\phi_1(-1) = 1, \quad \phi_2(1) = 0, \quad \phi_1(0) = \phi_2(0), \quad \frac{d\phi_1}{dy}(0) = \frac{d}{h} \frac{d\phi_2}{dy}(0). \quad (27)$$

First-order conditions

$$u_{11}(-1) = 0, \quad u_{21}(1) = 0, \quad u_{11}(0) = u_{21}(0), \quad (1 + \lambda_2) \frac{du_{11}}{dy}(0) = \frac{(1 + \lambda_1)}{mh} \frac{du_{21}}{dy}(0),$$

$$\theta_{11}(-1) = 1, \quad \theta_{21}(1) = 0, \quad \theta_{11}(0) = \theta_{21}(0), \quad \frac{d\theta_{11}}{dy}(0) = \frac{1}{kh} \frac{d\theta_{21}}{dy}(0). \quad (28)$$

Solutions for concentrations:

$$\varphi_1 = b_1 \text{Cosh}[\alpha_1 y] + b_2 \text{Sinh}[\alpha_1 y],$$

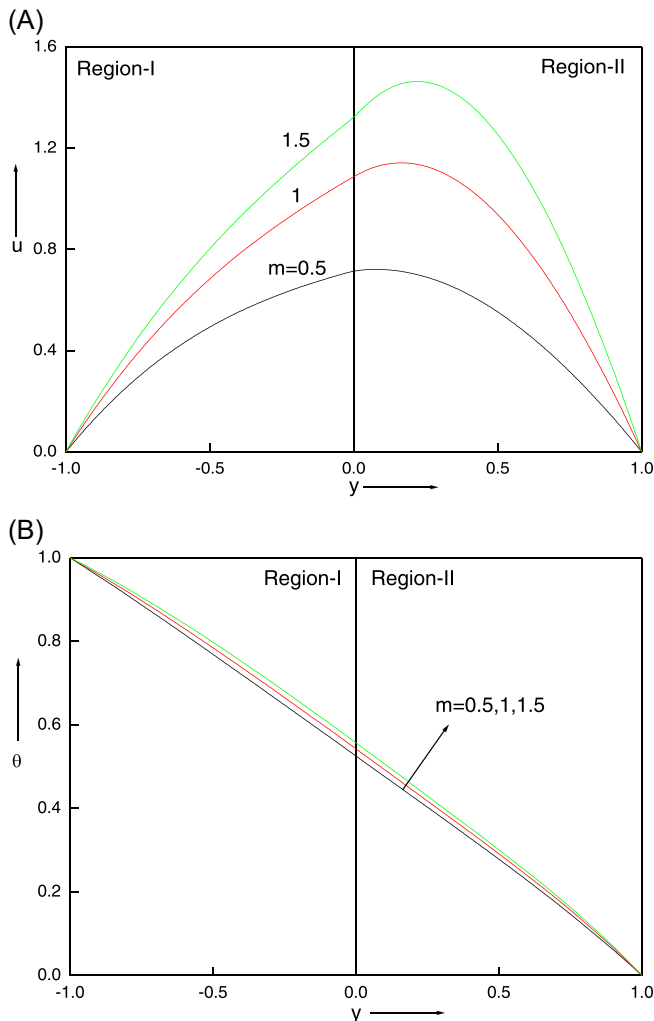


FIGURE 8 (A) Velocity profiles for different values of viscosity ratio  $m$ . (B) Temperature profiles for different values of viscosity ratio  $m$ . [Color figure can be viewed at [wileyonlinelibrary.com](http://wileyonlinelibrary.com)]

$$\varphi_2 = b_3 \text{Cosh}[\alpha_2 y] + b_4 \text{Sinh}[\alpha_2 y].$$

Solutions of the zeroth-order equations (17), (18), (22), and (23) using boundary conditions (27) are

$$\theta_{10} = c_1 y + c_2,$$

$$\theta_{20} = c_3 y + c_4,$$

$$u_{10} = A_2 + A_1 y + q_1 y^2 + q_2 y^3 + q_3 \text{Cosh}[\alpha_1 y] + q_4 \text{Sinh}[\alpha_1 y],$$

$$u_{20} = A_4 + A_3 y + q_5 y^2 + q_6 y^3 + q_7 \text{Cosh}[\alpha_2 y] + q_8 \text{Sinh}[\alpha_2 y]$$

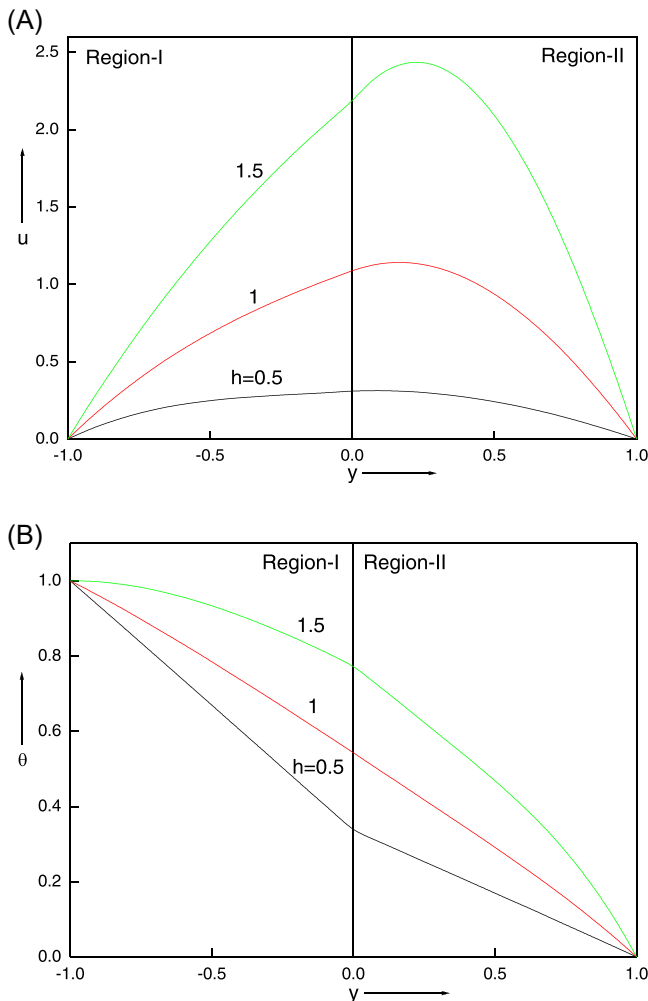
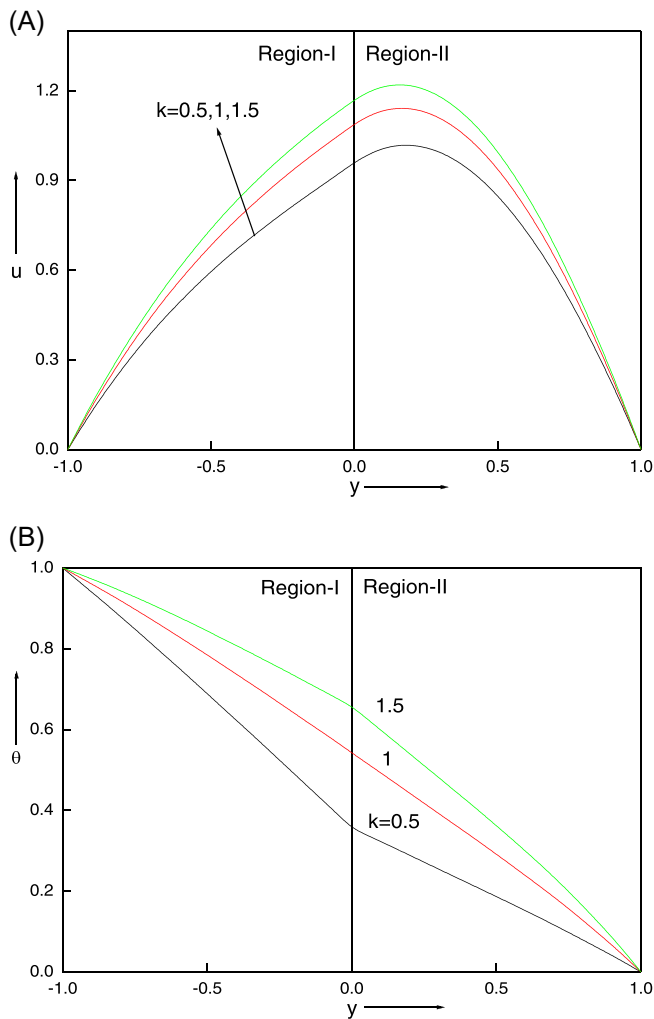


FIGURE 9 (A) Velocity profiles for different values of width ratio  $h$ . (B) Temperature profiles for different values of width ratio  $h$ . [Color figure can be viewed at [wileyonlinelibrary.com](https://onlinelibrary.wiley.com/doi/10.1002/ht.2204)]

The solutions of the first-order perturbation equations (20), (21), (25), and (26) using boundary conditions (28) are

$$\theta_{11} = A_6 + A_5 y + q_9 y^2 + q_{10} y^3 + q_{11} y^4 + q_{12} y^5 + q_{13} y^6 + q_{14} \text{Cosh}[\alpha_1 y] + q_{15} \text{Sinh}[\alpha_1 y] + q_{16} y \text{Cosh}[\alpha_1 y] + q_{17} y \text{Sinh}[\alpha_1 y] + q_{18} y^2 \text{Cosh}[\alpha_1 y] + q_{19} y^2 \text{Sinh}[\alpha_1 y] + q_{20} \text{Cosh}[2 \alpha_1 y] + q_{21} \text{Sinh}[2 \alpha_1 y],$$

$$\theta_{21} = A_8 + A_7 y + q_{22} y^2 + q_{23} y^3 + q_{24} y^4 + q_{25} y^5 + q_{26} y^6 + q_{27} \text{Cosh}[\alpha_1 y] + q_{28} \text{Sinh}[\alpha_1 y] + q_{29} y \text{Cosh}[\alpha_1 y] + q_{30} y \text{Sinh}[\alpha_1 y] + q_{31} y^2 \text{Cosh}[\alpha_1 y] + q_{32} y^2 \text{Sinh}[\alpha_1 y] + q_{33} \text{Cosh}[2 \alpha_1 y] + q_{34} \text{Sinh}[2 \alpha_1 y],$$



**FIGURE 10** (A) Velocity profiles for different values of thermal conductivity ratio  $k$ . (B) Temperature profiles for different values of thermal conductivity ratio  $k$ . [Color figure can be viewed at [wileyonlinelibrary.com](https://onlinelibrary.wiley.com)]

$$u_{11} = B_2 + B_1 y + T_1 y^2 + T_2 y^3 + T_3 y^4 + T_4 y^5 + T_5 y^6 + T_6 y^7 + T_7 y^8 + T_8 \text{Cosh}[\alpha_1 y] + T_9 \text{Sinh}[\alpha_1 y] + T_{10} y \text{Cosh}[\alpha_1 y] + T_{11} y \text{Sinh}[\alpha_1 y] + T_{12} y^2 \text{Cosh}[\alpha_1 y] + T_{13} y^2 \text{Sinh}[\alpha_1 y] + T_{14} \text{Cosh}[2\alpha_1 y] + T_{15} \text{Sinh}[2\alpha_1 y],$$

$$u_{21} = B_4 + B_3 y + T_{16} y^2 + T_{17} y^3 + T_{18} y^4 + T_{19} y^5 + T_{20} y^6 + T_{21} y^7 + T_{22} y^8 + T_{23} \text{Cosh}[\alpha_2 y] + T_{24} \text{Sinh}[\alpha_2 y] + T_{25} y \text{Cosh}[\alpha_2 y] + T_{26} y \text{Sinh}[\alpha_2 y] + T_{27} y^2 \text{Cosh}[\alpha_2 y] + T_{28} y^2 \text{Sinh}[\alpha_2 y] + T_{29} \text{Cosh}[2\alpha_2 y] + T_{30} \text{Sinh}[2\alpha_2 y].$$

## 4 | RESULTS AND DISCUSSION

The effects various parameters, namely, thermal Grashof number ( $2 \leq Gr_t \leq 10$ ), mass Grashof number  $2 \leq Gr_c \leq 10$ , thermal expansion coefficient ratio ( $b_t$ ), concentration expansion coefficient ratio ( $b_c$ ), Jeffrey parameter ( $1 \leq \lambda_1 \leq 3$ ), Jeffrey parameter ( $1 \leq \lambda_2 \leq 3$ ), viscosity ratio ( $m$ ), width ratio ( $h$ ), thermal conductivity ( $k$ ), diffusion coefficient ratio ( $d$ ), chemical reaction parameter ( $\alpha$ ), and pressure ( $P$ ) in a vertical channel for the fluid velocity ( $v$ ), temperature ( $\theta$ ), and concentrations ( $\varphi$ ) are evaluated analytically using the regular perturbation method for the small values of  $\varepsilon$  as perturbation parameter and the results are depicted graphically.

Figures 2A,B and 3A,B describe the increase in the velocity and temperature profile by increasing the thermal and mass Grashof number. Physically increase in the Grashof number increases the buoyancy as a result flow increases in both regions due to the increase in viscous power.

From Figures 4A,B and 5A,B, it appears that an increase in the coefficient of thermal expansion ratio  $b_t$  and concentration expansion coefficient ratio  $b_c$  enhances the fluid flow behavior on the velocity and temperature fields, and temperature profiles improve with varying the coefficient of thermal expansion  $b_t$  and  $b_c$ .

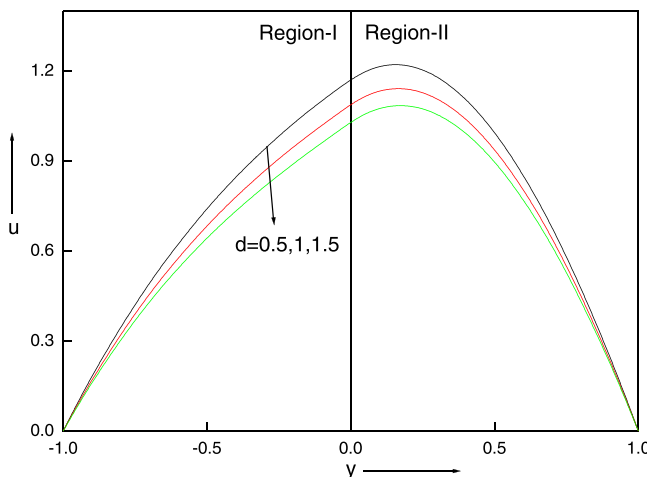


FIGURE 11 Velocity profiles for different values of diffusion coefficient ratio  $d$ . [Color figure can be viewed at [wileyonlinelibrary.com](https://onlinelibrary.wiley.com/doi/10.1002/htj.22094)]

Statistics show that with a Jeffrey parameter variation, velocity, and temperature profiles increase with increasing values of Jeffrey parameters  $\lambda_1$  and  $\lambda_2$  as shown in Figures 6A,B and 7A,B, respectively, it is due to the ratio of relaxation to retardation time. Also, it is noticed that the dimensionless fluid velocity has a higher value for a Newtonian fluid ( $\lambda_1 = \lambda_2 = 0$ ) than that for the non-Newtonian fluid.

Figure 8A,B portrays that the velocity and temperature profiles enhance the flow for the various values of viscosity ratio  $m$ , for  $m = 0.5$  here the fluid is very clear and has the viscosity twice the first region as compared to the second region due to this reason we see the various amplitudes in both regions.

Average width  $h = 5$ , an increase in the width ratio enhances the fluid flow in both regions, represented in Figure 9A,B.

As the conductivity ratio increases, they get more heat and start bombarding each other as a result their flow enhances both velocity and temperature profiles which are shown in Figure 10A,B.

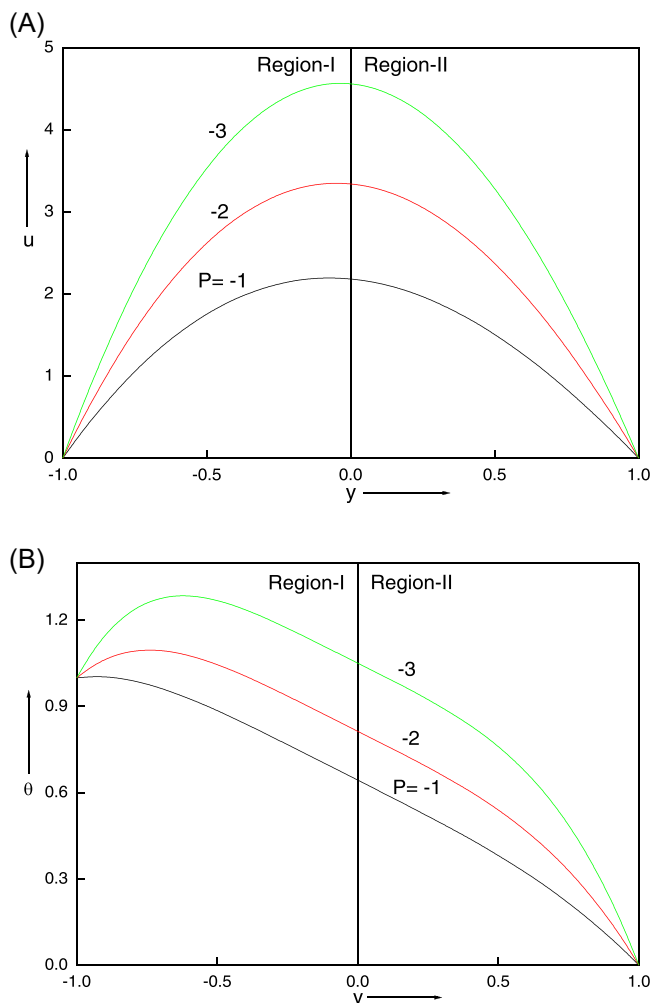


**FIGURE 12** (A) Velocity profiles for different values of pressure gradient  $P$ . (B) Temperature profiles for different values of pressure gradient  $P$ . [Color figure can be viewed at [wileyonlinelibrary.com](https://wileyonlinelibrary.com)]

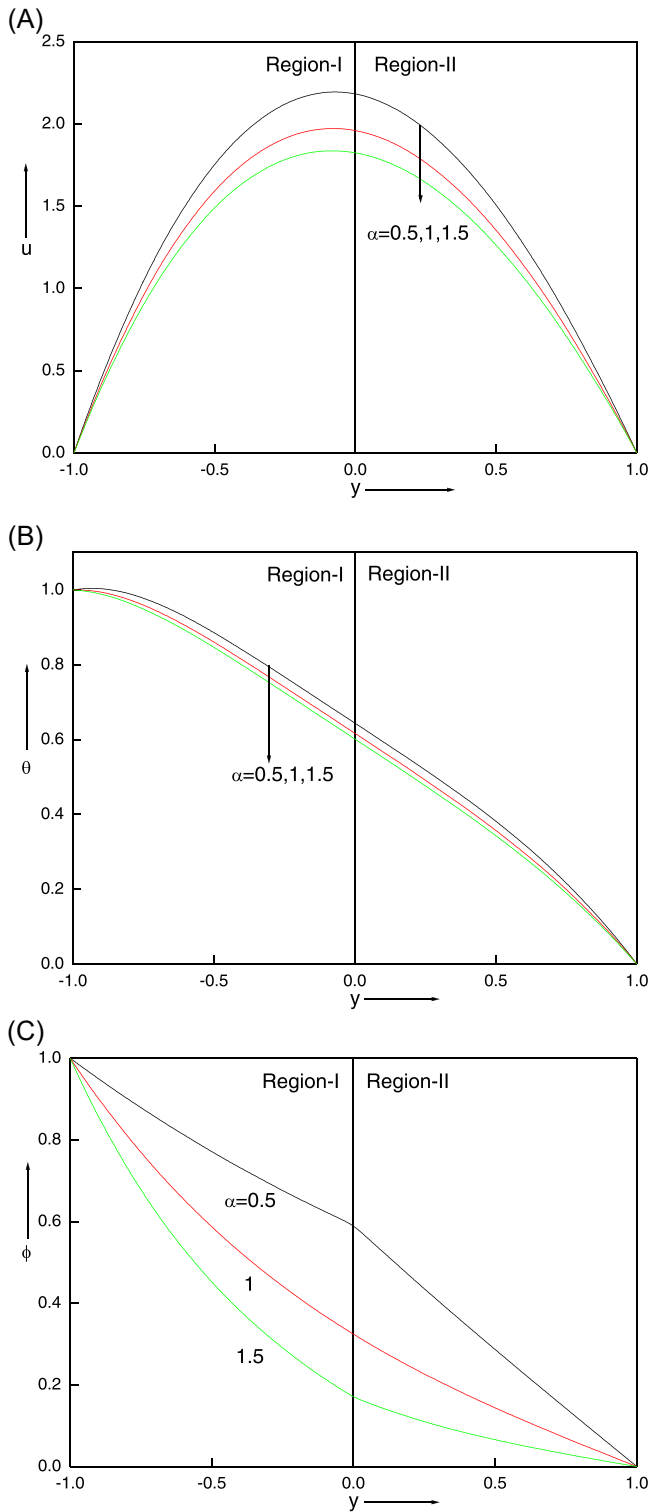


**FIGURE 13** (A) Velocity profiles for different values of chemical reaction parameter  $\alpha$ . (B) Temperature profiles for different values of chemical reaction parameter  $\alpha$ . (C) Concentration profiles for different values of chemical reaction parameter  $\alpha$ . [Color figure can be viewed at [wileyonlinelibrary.com](https://wileyonlinelibrary.com)]

Differences in diffusion coefficient ratio  $d$  suppress the fluid flow behavior because of diffusivity, as shown in Figure 11.

Figure 12A,B describes the variation in pressure gradient  $P$  values, increasing the velocity and temperature profiles in both regions.

Figure 13A–C represents that the variation in the chemical reaction parameter  $\alpha$  affects the field of velocity, temperature, and concentration profiles. Physically increase in concentration increases the solute molecules as a result it suppresses the fluid flow in both regions.

Also, it is established that the Nusselt number is boosted by enhancing the thermal, and mass Grashof numbers shown in Figures 14 and 15. Nusselt number enhances its magnitude at

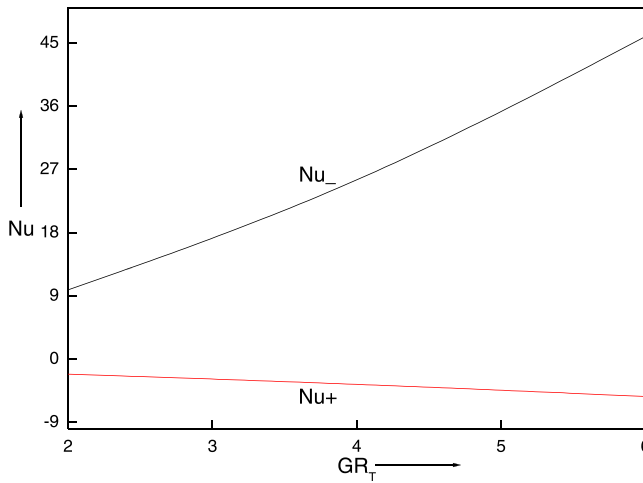


FIGURE 14 Effect of thermal Grashof number on the Nusselt number. [Color figure can be viewed at [wileyonlinelibrary.com](https://onlinelibrary.wiley.com/doi/10.1002/htj.22094)]

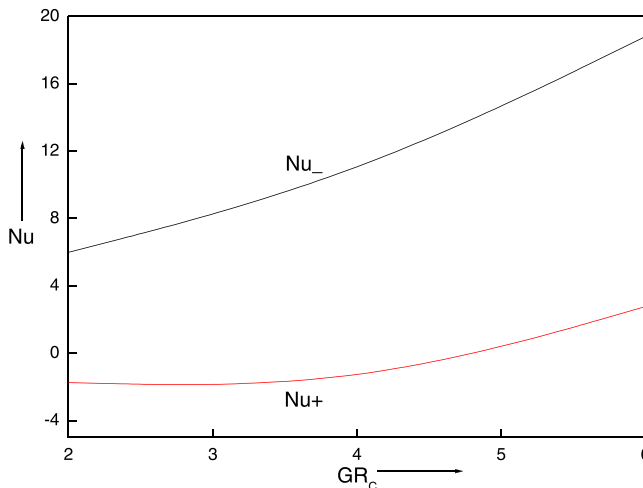


FIGURE 15 Effect of mass Grashof number on the Nusselt number. [Color figure can be viewed at [wileyonlinelibrary.com](https://onlinelibrary.wiley.com/doi/10.1002/htj.22094)]

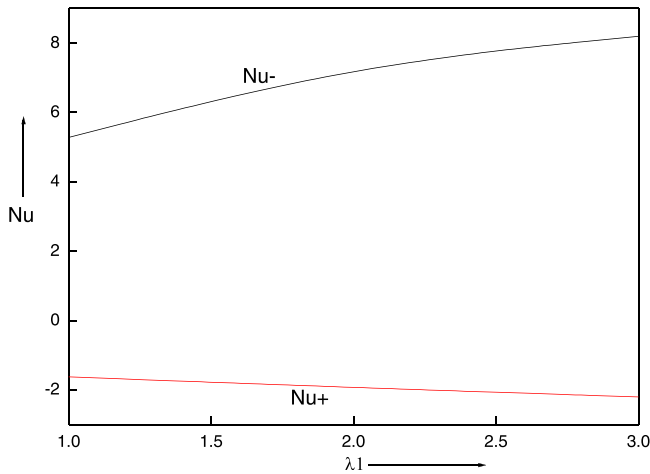


FIGURE 16 Effect of Jeffrey parameter on the Nusselt number. [Color figure can be viewed at [wileyonlinelibrary.com](http://wileyonlinelibrary.com)]

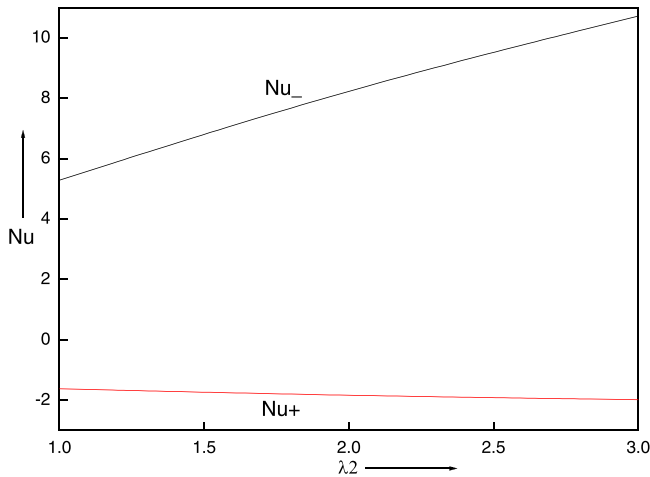


FIGURE 17 Effect of Jeffrey parameter on the Nusselt number. [Color figure can be viewed at [wileyonlinelibrary.com](http://wileyonlinelibrary.com)]

cold wall  $Nu_-$  and hot walls  $Nu_+$ . From Figures 16 and 17 we noticed that the different values of Jeffrey parameters as Nusselt number increases at both hot and cold walls.

## 5 | CONCLUSION

In this paper, we have investigated the heat and mass transfer of two immiscible flows of Jeffrey fluid in a vertical channel in the presence of chemical reaction parameters and governing equations are solved analytically by using the regular perturbation method. The main points of this analysis are given below:

1. As  $Gr_t$  and  $Gr_c$  increase it enhances the fluid flow nature because of the buoyancy force to the viscous force which supports the motion.
2. The effects of Jeffrey's parameters with high values in velocity and temperature range are rising in both the region due to its comfort and delay structure. Physically, an increase in  $\lambda$  means a reduction in fluid retardation time which in turn stops the hastening of fluid motion. On the other hand, the temperature profile increases with the increase of  $\lambda$  which is obvious from Figure 5B. Physically, an increase in  $\lambda$  leads to a rise in relaxation time and diminish in retardation time, due to this higher temperature and thicker thermal boundary layer.
3. At different diffusion coefficient ratios, it reduces the velocity profile in both regions.
4. The effect of the chemical reaction parameter suppresses the fluid flow nature in velocity, temperature, and concentration.
5. Increasing the values of  $Gr_t$ ,  $Gr_c$ , and Jeffery parameters increases the Nusselt number near the cold wall and hot wall.

## DATA AVAILABILITY STATEMENT

The data that support the findings of this study are available on request from the corresponding author. The data are not publicly available due to privacy or ethical restrictions.

## NOMENCLATURE

$b_c$	ratio of concentration expansion ( $\alpha_1, \alpha_2$ )
$Br$	Brinkman number [ $\bar{U}_1^2 \mu_1 / K_1 (T_{w1} - T_{w2})$ ]
$b_t$	ratio of thermal expansion ( $\beta_{T2} / \beta_{T1}$ )
$C_1, C_2$	concentrations
$\bar{C}_1, \bar{C}_2$	reference concentrations
$d$	ratio of diffusion coefficient ( $D_2 / D_1$ )
$D_1, D_2$	diffusion coefficients
$Gc$	modified Grashof number ( $g \beta_{C1} \Delta C h_1^3 / \nu_1^2$ )
$Gr$	Grashof number ( $g \beta_{T1} \Delta T h_1^3 / \nu_1^2$ )
$Gr_c$	mass Grashof number ( $Gc / Re$ )
$Gr_t$	thermal Grashof number ( $Gr / Re$ )
$g$	acceleration due to gravity
$h_1, h_2$	width of two regions
$k$	thermal conductivity ratio ( $K_1 / K_2$ )
$K_1, K_2$	thermal conductivities
$m$	viscosities ratio ( $\mu_1 / \mu_2$ )
$n$	density ratio ( $\rho_2 / \rho_1$ )
$P$	pressure gradient [ $P = h_1^2 / (\mu_1 \bar{U}_1) (dp / dX)$ ]
$Re$	Reynolds number ( $\bar{U}_1 h_1 / \nu_1$ )
$T_1, T_2$	temperatures
$T_{w1}, T_{w2}$	temperatures at the boundaries
$\bar{U}_1$	reference velocity

## GREEK SYMBOLS

$\alpha_1, \alpha_2$	chemical reaction parameters
$\beta_{C1}, \beta_{C2}$	concentration expansions coefficients
$\beta_{T1}, \beta_{T2}$	thermal expansions coefficients

$\Delta T, \Delta C$	difference in temperature and concentration
$\lambda_1, \lambda_2$	Jeffrey parameters in R-I, II
$\mu_1, \mu_2$	viscosities
$\nu_1, \nu_2$	kinematic viscosities
$\varphi_1, \varphi_2$	nondimensional concentrations
$\theta$	nondimensional temperature $[(T - T_{w2}) / (T_{w1} - T_{w2})]$

## SUBSCRIPTS

$i = 1, 2$  reference quantities for Region-I and Region-II, respectively

## CONFLICT OF INTEREST

The authors declare no conflict of interest.

## ORCID

Shreedevi Kalyan  <http://orcid.org/0000-0001-8270-4324>

## REFERENCES

- Hayat T, Ali N, Asghar S, Siddiqui AM. Exact peristaltic flow in tubes with an endoscope. *Appl Math Comput.* 2006;182:359-368.
- Vajravelu K, Sreenadh S, Lakshminarayana P. The influence of heat transfer on peristaltic transport of a Jeffrey fluid in a vertical porous stratum. *Commun Nonlinear Sci Numer Simul.* 2011;16:3107-3125.
- Jyothi KL, Devaki P, Sreenadh S. Pulsatile flow of a Jeffrey fluid in a circular tube having internal porous lining. *Int J Math Arch.* 2013;4:75-82.
- Kothandapani M, Srinivas S. Peristaltic transport of a Jeffrey fluid under the effect of magnetic field in an asymmetric channel. *Int J Non-linear Mech.* 2008;43:915-924.
- Pandey SK, Tripathi D, Fang T. Unsteady model of transportation of Jeffrey-fluid by peristalsis. *Int J Biomath.* 2010;3:473-491.
- Santhosh N, Radhakrishnamacharya G, Chamkha AJ. Flow of a Jeffrey fluid through a porous medium in narrow tubes. *J Porous Media.* 2015;18(1):71-78.
- Anu Nair P, Karuppasamy K, Benziger B, Balkrishnan P. Natural convective heat transfer from horizontal heated plate facing upward in vertical channel—a review. *Int J Mech Eng Res.* 2015;5(1):27-38.
- Anu Nair P, Karuppasamy K. Comparative study of Bayesian approach and least square residual optimization method in horizontal heated plate facing upward—an experimental approach. *Int J Res Aeronaut Mech Eng.* 2015;3(4):7-18.
- Anu Nair P, Elias S, John V, Amboori RK. An inexpensive technique to determine the parameter in free convection heat transfer from two parallel heated vertical plates. *Eur J Adv Eng Technol.* 2015;2(10):49-55.
- Anu Nair P, Abraham AK, Premjith S. Optimal location of discrete heat sources on and inside a wall with natural convection. *Int J Appl Eng Res.* 2015;10(20):41205-41211.
- Anu Nair P, Karuppasamy K. Experimental approach of natural convection heat transfer in vertical channel with horizontal heated plate at small height ratio. *Asian J Eng Technol.* 2015;3(4):316-325.
- Ebenezer M, Rajkumar MR, Chandramohan Nair PS. Determination of hot spot temperature of a single phase transformer subjected to harmonic pollution. *J Inst Eng India Ser B.* 2012;93(3):143-149.
- Bird RB, Armstrong RC, Hassager O. Dynamics of polymeric liquids. In: *Fluid Mechanics*. Vol 1. A Wiley inter science publication, John Wiley and sons; 1977.
- Hayat T, Ali N, Asghar S. An analysis of peristaltic transport for flow of a Jeffrey fluid. *ActaMach.* 2007;193: 101-112.
- Nallapu S, Radhakrishnamacharya G. Jeffrey fluid flow through porous medium in the presence of magnetic field in narrow tubes. *Int J Sci Eng Res.* 2014;4(11):468-473.

16. Maqbool K, Shaheen S, Mann AB. Exact solution of cilia induced flow of a Jeffrey fluid in an inclined tube. *Springer Plus*. 2016;5:1379.
17. Chandrasekhar Reddy K, Sudhakara E. Fully developed free convective flow of a Jeffrey fluid in a circular pipe. *Int J Adv Eng Res Dev*. 2017;4(9):217-224.
18. Aly AM, El-Sapa S. Double rotations of cylinders on thermo solutal convection of a wavy porous medium inside a cavity mobilized by a nanofluid and impacted by a magnetic field, AM Aly, S El-Sapa. *Int J Numer Methods Heat Fluid Flow*. 2022;32:1-24. ISSN: 0961-5539.
19. Aly AM, El-Sapa S. Effects of Soret and Dufour numbers on MHD thermosolutal convection of a nanofluid in a finned cavity including rotating circular cylinder and cross shapes, AM Aly, S El-Sapa. *Int Commun Heat Mass Transfer*. 2022;130:105819.
20. Tayebi T, Dogonchi AS, Chamkha AJ, Hamida MBB, El-Sapa S, Galal AM. Micropolar nanofluid thermal free convection and entropy generation through an inclined I-shaped enclosure with two hot cylinders. *Case Stud Therm Eng*. 2022;31:101813.
21. Nayak MK, Karimi N, Chamkha AJ, Dogonchi AS, El-Sapa S, Galal AM. Efficacy of diverse structures of wavy baffles on heat transfer amplification of double-diffusive natural convection inside a C-shaped enclosure filled with hybrid nanofluid. *Sustainable Energy Technol Assess*. 2022;52:102180.
22. Qasim M, Afridi MI, Wakif A, Saleem S. Influence of variable transport properties on nonlinear radioactive Jeffrey fluid flow over a disk: utilization of generalized differential quadrature method. *Arab J Sci Eng*. 2019;44(6):5987-5996.
23. Prathap Kumar J, Umavathi JC, Chamkha Ali J, Pop I. Fully developed free convective flow of micropolar and viscous fluids in a vertical channel. *Appl Math Model*. 2010;34:1175-1186.
24. Liao SJ. On the analytic solution of magneto hydrodynamic flows of non-Newtonian fluids over a stretching sheet. *J Fluid Mech*. 2003;488:189-212; Liao SJ. On the homotopy analysis method for nonlinear problems. *Appl Math Comput*. 2004;147:499-513.
25. Cheng J, Liao SJ, Pop I. Analytic series solution for unsteady mixed convection boundary layer flow near the stagnation point on a vertical surface in porous medium. *Transp Porous Media*. 2005;61:365-379.
26. Liao SJ, Magyari E. Exponentially decaying boundary layers as limiting cases of families of algebraically decaying ones. *Math Phys*. 2006;57:777-792.
27. He JH, Shou DH. Application of parameter-expanding method to strongly nonlinear oscillators. *Int J Non-Linear Sci Numer Simul*. 2007;8:121-124.
28. Sajid M, Abba Z, Hayat T. Homotopy analysis for boundary layer flow of a micropolar fluid through a porous channel. *Appl Math Model*. 2009;33(11):4120-4125.
29. Malashetty MS, Umavathi JC, Prathapkumar J. Magneto convection of two immiscible fluids in vertical enclosure. *Heat Mass Transfer*. 2006;42:977-993.
30. Hayat T, Khan M, Asghar S. Homotopy analysis of MHD flows of an Oldroyd8constant fluid. *Acta Mech*. 2004;168:213-231.
31. Wu W, Liao SJ. Solving solitary waves with discontinuity by mean of the homotopy analysis method. *Chaos Solitons Fractals*. 2005;26:177-185.
32. Abbasband S. The application of homotopy analysis method to nonlinear equations arising in heat transfer. *Phys Lett A*. 2006;360:109-113.
33. Xu H, Liao S-J, Pop I. Series solution of unsteady boundary layer flows of non-Newtonian fluid near a forward stagnation point. *J Non-Newtonian Fluid Mech*. 2006;139:31-43.
34. Sajid M, Hayat T, Asghar S. Comparison of the HAM and HPM solutions of thin film flow of non-Newtonian fluids on a moving belt. *Nonlinear Dyn*. 2007;50:27-35.
35. Jiao X, Gao Y, Lou S. Approximate homotopy symmetry method: homotopy series solutions to the sixth-order Boussinesq equation. *Sci China Ser G: Phys Mech Astronomy*. 2009;52:1169-1178.
36. Zhu J, Zheng L, Zhang X. Analytical solution to stagnation-point flow and heat transfer over a stretching sheet based on homotopy analysis. *Appl Math Mech*. 2009;30:463-474.
37. Harish Babu D, Satya Narayana PV. Joule heating effects on MHD mixed convection of a Jeffrey fluid over a stretching sheet with power law heat flux: a numerical study. *J Magn Magn Mater*. 2016;412:185-193.
38. Satya Narayana PV, Harish Babu D. Numerical study of MHD heat and mass transfer of a Jeffrey fluid over a stretching sheet with chemical reaction and thermal radiation. *J Taiwan Inst Chem Eng*. 2016;59:18-25.

39. Harish Babu D, Satya Narayana PV. Influence of variable permeability and radiation absorption on heat and mass transfer in MHD micropolar flow over a vertical moving porous plate. *Research Article Open Access*, Volume 2013. Article ID 953536, doi:10.1155/2013/953536.Dondu
40. Babu Harish D, Tarakaramu N, Satya Narayana PV, Sarojamma G, Makinde OD. MHD flow and heat transfer of a Jeffrey fluid over a porous stretching/shrinking sheet with a convective boundary condition. *Int J Heat Technol.* 2021;39(3):885-894.
41. Kumaraswamy Naidu K, Harish Babu D, Harinath Reddy S, Satya Narayana PV. Radiation and partial slip effects on magnetohydrodynamic Jeffrey nanofluid containing gyrotactic microorganisms over a stretching surface. *J Therm Sci Eng Appl.* 2021;13(3):031011(11 pages) Paper No. TSEA 20-031362. doi:10.1115/1.4048213
42. Harish Babu D, Ajmath KA, Venkateswarlu B, Satya Narayana PV. Thermal radiation and heat source effects on MHD non-Newtonian nanofluid flow over a stretching sheet. *J Nanofluids.* 2018;8(5):1085-1092. doi:10.1166/jon.2019.1666
43. Harish Babu D, Satya Narayana PV. Melting heat transfer and radiation effects on Jeffrey fluid flow over a continuously moving surface with a parallel free stream. *Appl Comput Mech.* 2019;5(2): 468-476. doi:10.22055/JACM.2019.26479.1335

**How to cite this article:** Kalyan S, Sharan A, Chamkha AJ. Heat and mass transfer of two immiscible flows of Jeffrey fluid in a vertical channel. *Heat Transfer.* 2022;1-22. doi:10.1002/htj.22694